2024 IEEE 63rd Conference on Decision and Control (CDC)
December 16-19, 2024. MiCo, Milan, Italy

Advanced Safety Filter for Smooth Transient Operation of a Battery Energy Storage System

Michael Schneeberger, Florian Dörfler, Silvia Mastellone

Abstract— **This paper presents an advanced safety filter based on Control Barrier and Control Lyapunov Functions to smoothly limit the current of an inverter-based Battery Energy Storage System, avoiding converter tripping, operational loss, and potential component failure. The task involves finding Control Barrier and Control Lyapunov Function via Sum-of-Squares optimization to ensure feasibility of the safety filter at every state along the trajectory. We showcase the effectiveness of the implementation through simulations involving a load step at the Point of Common Coupling, and we compare the outcomes with those obtained using a standard vector current controller.**

I. Introduction

A Battery Energy Storage System (BESS) enables part of the power grid to disconnect from the utility grid and operate independently in an islanded mode. In this scenario, the primary objective of the BESS is to maintain grid voltage and frequency stability through the use of an inert grid-forming (GFM) control scheme. However, when operating in grid-connected mode, the BESS's current needs to be limited during transient grid events such as faults, load steps or changes in configuration to protect the system's hardware and prevent operational loss. In such situations, a fast response is necessary to ensure the system's safety.

In a microgrid configuration, a compelling GFM control scheme is the Enhanced Direct Power Control (EDPC) [1], [2]. One version of this approach, described in [3], consists of an active and reactive power controller that, together with a feed-forward term derived from a filtered voltage measurement at the Point of Common Coupling (PCC), determines the converter voltage reference. In islanding configuration, the EDPC operates in GFM mode due to the slow dynamics of this filtered PCC voltage. However, during transients, faster filtered PCC voltage dynamics are temporarily permitted, even at the expense of potentially sacrificing the GFM property, to facilitate a stable return to EDPC operation.

To limit the converter current in grid-connected mode, a vector current controller can be activated based on a grid fault detection [4]. However, this requires manually tuning (assuming a worst-case fault) the control gains of the current controller to respect the current limits and often causes undesired chattering behaviors resulting from the activation and deactivation of the current controller. Current limiting strategies based on limiting the current reference, or introducing virtual impedance have been proposed [5], [6]. In this approach, unlike the EDPC, a vector current control is an integral part of the GFM control scheme, rendering any switching action obsolete. None of these approaches provide a safety certification for the BESS across all states.

In this paper, we employ a *safety filter* approach to limit the current and achieve a smooth transition between operation under EDPC and current limiting control. Traditionally, the safety filter is obtained by solving a Quadratic Program (QP) at every state, based on a Control Barrier Function (CBF) and an internal system model, to ensure the system remains within the *safe set*, as described in [7]. The safety filter can also incorporate a linear constraint that encodes the Control Lyapunov Function (CLF) condition, ensuring not only safety but also convergence to a specific set [8]. To ensure feasibility of the QP for all states along the trajectory, polynomial CBF and CLF candidates can be numerically derived by solving a series of Sum-of-Squares (SOS) optimization problems [9], [10]. Furthermore, linear input constraints can be included in both the QP and the SOS constraints during CBF and CLF searches [11], [12].

In our previous work, we proposed an advanced safety filter [13], that extends the basic version by ensuring a finite-time convergence to a forward invariant set, referred to as *nominal region*, wherein the nominal controller remains undisturbed by the safety filter. In this work, we apply this concept to the BESS control scenario, leveraging the convergence guarantee to return the system to the GFM operation of the EDPC within a finite amount of time. Maintaining undisturbed operation during nominal conditions is crutial, as the safety filter could otherwise interfere with the GFM behavior of the EDPC. The advanced safety filter is implemented using a Quadratically Constrained Quadratic Program (QCQP), providing the capability to encode the quadratic input constraints.

We extended the resuls from our previous work in [13], by introducing several improvements to reduce the conservativeness and enhance the robustness of the advanced safety filter, making it more practically applicable to BESS converter control in complex, dynamic grid environments. These improvements include creating a margin between the safe set and the state constraints, and trading off the volume of the nominal region with a slightly more aggressive control response near the boundary of the safe set through

Michael Schneeberger and Silvia Mastellone are with the Institute of Electrical Engineering, FHNW, Windisch, Switzerland (e-mails: michael.schneeberger@fhnw.ch, silvia.mastellone@fhnw.ch), and Florian Dörfler is with the Department of Information Technology and Electrical Engineering, ETH Zürich, Switzerland, (e-mail: dorfler@control.ee.ethz.ch)

This work was supported by the Swiss National Science Foundation (SNSF) under NCCR Automation.

adjustments of the SOS constraints. Furthermore, to ensure the existence of a CLF that satisfies the safety and finite-time convergence condition, we integrate the dynamics of the filtered PCC voltage into the internal system model of the safety filter. Finally, we demonstrate the effectiveness of the proposed solution through simulations where a load step is applied at the Point of Common Coupling (PCC). The system response is compared with the one obtained using a standard vector current controller. This study demonstrates the applicability and efficacy of the safety filter concept in a non-trivial power electronics example beyond its traditional application in robotics.

The remainder of the paper is structured as follows: Section II describes the problem setup including the BESS, the EDPC, and the requirement on the current limiting control. In Section III, we present the concept of the advanced safety filter, its properties, and the resulting SOS formulation. Numerical results, presented in Section IV, demonstrate the superior performance of the safety filter in comparison to a conventional vector current control [4]. Finally, Section V concludes the paper.

II. Battery Energy Storage System

A. Problem setup

Consider a BESS implemented as a three-phase power inverter system connected to the PCC through a transformer, as depicted in Figure 1. Given that the state of charge (SOC) of the BESS's battery changes at a much slower rate than the control, we model it as a constant dc-voltage source v_{dc}. A grid filter installed between transformer and PCC, along with an optimized pulse pattern (OPP), suppresses high-frequency harmonics generated by the inverter modulation. This supports the use of an averaged inverter model, in which the output voltage of the BESS converter is expressed as the product of the dc-link voltage $v_{dc} \in \mathbb{R}$ and the modulation index $m := \begin{bmatrix} m_d & m_q \end{bmatrix}^\top \in \mathbb{R}^2$. The converter voltage $v_c \in \mathbb{R}^2$ is thus given by:

$$v_c := v_{dc} m,$$

where m is constrained by $m^{\max} \in \mathbb{R}$:

$$m_d^2 + m_q^2 \leq (m^{\max})^2 . \tag{1}$$

Since the controller's bandwidth is significantly slower than the frequency range of the grid filter, we simplify the grid filter model by representing it as a single inductance. Similarly, the transformer, which steps up the voltage to match the grid voltage at the PCC, is represented by a single inductance. The current dynamics over the filter and transformer inductance l_c in p.u. are expressed as

$$\frac{l_c}{\omega_n} \begin{bmatrix} \dot{i}_d \\ \dot{i}_q \end{bmatrix} = -Z_c \underbrace{\begin{bmatrix} i_d \\ i_q \end{bmatrix}}_{=:i} - \underbrace{\begin{bmatrix} v_{\mathrm{PCC},d} \\ v_{\mathrm{PCC},q} \end{bmatrix}}_{=:v_{\mathrm{PCC}}} + \underbrace{\begin{bmatrix} v_{c,d} \\ v_{c,q} \end{bmatrix}}_{=:v_c}, \tag{2}$$

where $\omega_n := 2\pi 50\mathrm{Hz}$ represents the nominal grid frequency, and the current i and voltage v_{PCC} are measured as shown in Figure 1. $Z_c := J\omega l_c$ denotes the matrix representation

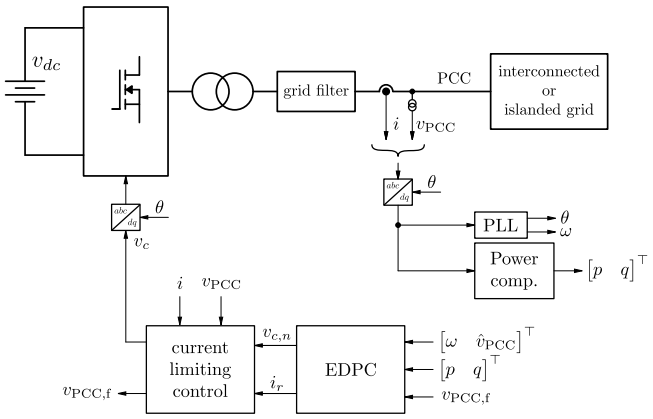

Fig. 1. The BESS is implemented as a three-phase power inverter system connected to the PCC via a transformer and a grid filter. The EDPC in series with a current limiting control ensures GFM behavior during islanded grid operation while limiting the current during grid transients.

of the combined filter and transformer inductance with $J = \left[\begin{smallmatrix} 0 & -1 \\ 1 & 0 \end{smallmatrix}\right]$. The precise value of l_c is determined during the commissioning of the BESS.

Operating the BESS in both grid-connected and islanding modes, requires suitable control strategies that meet grid stability and load requirements. The BESS control architecture consist of two main components. The slow outer loop, in form of the EDPC, is responsible for meeting the grid stability and load requirements, while the fast inner loop, in form of a current limiting controller, is designed to limit the current during transients.

B. Enhanced Direct Power Control

The EDPC, as described in [1], [2], [3] and illustrated in Figure 2, consists of an active and reactive power loop. It achieves a slow time constant through the utilization of a low-pass filter in the measurement of active power p and reactive power q. The active and reactive power references are determined by a frequency droop $D_f \in \mathbb{R}$ and a voltage droop $D_v \in \mathbb{R}$c, respectively:

$$p_r := D_f(\omega - 1) \quad q_r := D_v(\hat{v}_{\mathrm{PCC,LP}} - 1), \tag{3}$$

where ω is the angular frequency of the PLL in p.u., and $\hat{v}_{\mathrm{PCC,LP}}$ is the low-pass filtered PCC voltage amplitude. The active and reactive power control, depicted in Figure 2, are based on the PI controller

$$K_p \left(1 + \frac{1}{T_i s}\right), \tag{4}$$

characterized by a proportional gain $K_p \in \mathbb{R}$ and integral time constant $T_i \in \mathbb{R}$. This controller transforms the active and reactive power error into a (nominally unlimited) current reference. A current reference limiter

$$\|i_r\|^2 = i_{r,d}^2 + i_{r,q}^2 \leq (i_r^{\lim})^2 \tag{5}$$

for some current reference limit $i_r^{\lim}$ that ensures a stable steady-state current below the maximum allowed converter current $i^{\max}$ defined in (9). A cross-coupling term Z_c

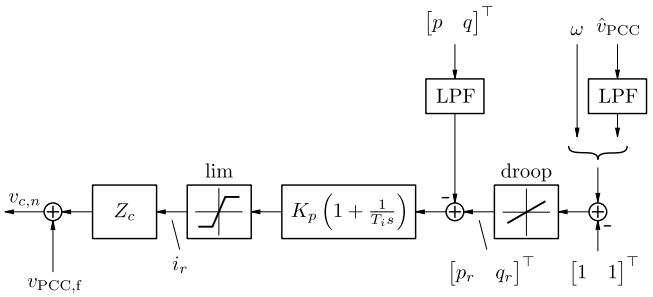

Fig. 2. The Enhanced Direct Power Control (EDPC) directly generates a converter voltage reference $v_{c,n}$ from a power control loop.

computes the voltage drop over the transformer and grid filter impedance. Finally, a filtered PCC voltage $v_{\mathrm{PCC},f}$ is added to the voltage drop, producing the BESS's voltage

$$v_{c,n} := Z_c i_r + v_{\mathrm{PCC},f}. \tag{6}$$

The dynamical system characterizing the filtered PCC voltage is given as

$$\underbrace{\begin{bmatrix}\dot{v}_{\mathrm{PCC},f,d}\\ \dot{v}_{\mathrm{PCC},f,q}\end{bmatrix}}_{=:\dot{v}_{\mathrm{PCC},f}} = \underbrace{\begin{bmatrix}\alpha_d\\ \alpha_q\end{bmatrix}}_{=:\alpha}, \tag{7}$$

where $\alpha \in \mathbb{R}^2$ is the input of this system. To achieve GFM behavior, the filtered PCC voltage must exhibit characteristics of a low-pass filter with time constant $\tau \approx 100ms$. This is achieved through the following nominal input:

$$\alpha_n := \frac{v_{\mathrm{PCC}} - v_{\mathrm{PCC},f}}{\tau}. \tag{8}$$

To maintain the GFM property, deviation from the nominal input are only allowed during transients.

C. The problem of current limiting control

The current limiting control at the output of the EDPC, as shown in Figure 1, ensures that the current stays within the maximum allowed boundaries, characterized by $i^{\max} \in \mathbb{R}$:

$$i_d^2 + i_q^2 \leq (i^{\max})^2. \tag{9}$$

This is achieved by adjusting the nominal voltage reference $v_{c,n}$ (6) to generate a safe voltage reference v_c. Furthermore, the dynamics governing the filtered PCC voltage $v_{\mathrm{PCC},f}$ in (7) and (8) can be temporarily adjusted during a current transient, facilitating a stable return to EDPC operation.

The design of the current limiting control and later of the advanced safety filter is based on a grid model, which in practice can be of arbitrarily complexity and subject to change over time. Moreover, the original models used for the EDPC have an unrequired degree of complexity. Therefore, we introduce the following simplifying assumptions:

- First, we adopt a simplified reduced-order grid model based on the current dynamics (2), where v_{PCC} is assumed to be constant in dq reference frame.
- Second, we propose a simplified reduced-order EDPC model based on (6), where the current reference i_r is assumed to be constant.

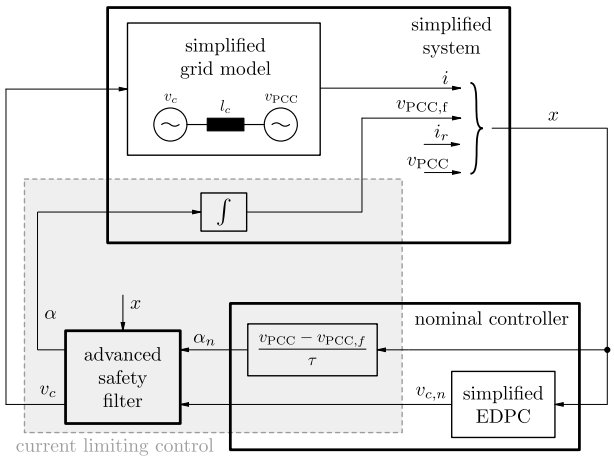

Fig. 3. The advanced safety filter ensures safe operation of the BESS with respect to the maximum allowed current limits (9).

Under those assumptions, we can formulate the problem statement as follows:

Problem 1: Given the dynamical system described in (2) and (7), with a constant voltage source v_{PCC}, a set of allowable states (9), an input constraint set (12), and a nominal controller described in (6) and (8), with a constant current reference i_r, the task is to design an advanced safety filter, as described in [13], that ensures stable and safe behavior of the BESS during grid events.

A standard method to solve Problem 1 is to employ a vector current control [4]. This involves a PI controller integrated with an anti-windup mechanism. However, this leads to chattering effects, abrupt behavior, and possibly system shutdown in case of protection function activation.

III. Advanced safety filter

To overcome the limitations of the state of the art vector current controller, we propose an alternative solution that allows to promptly respond to grid events while guaranteeing a smooth transitioning between EDPC and current limiting operation. This entails designing an advanced safety filter, as shown in Figure 3, to enforce the state and input constraints while ensuring finite-time convergence to the EDPC operation through the use of a CLF condition.

Consider the control system composed of the simplified grid model derived from (2), the filtered PCC voltage dynamics derived from (7), as well as the stationary dynamics of the current reference i_r and PCC voltage v_{PCC} as follows:

$$\dot{x} = \underbrace{\begin{bmatrix}-(\omega_n/l_c)\left(Z_c i + v_{\mathrm{PCC}}\right)\\ 0\\ 0\\ 0\end{bmatrix}}_{=:f(x)} + \underbrace{\begin{bmatrix}(\omega_n/l_c)\mathrm{I}_2 & 0\\ 0 & \mathrm{I}_2\\ 0 & 0\\ 0 & 0\end{bmatrix}}_{=:G(x)} \underbrace{\begin{bmatrix}v_c\\ \alpha\end{bmatrix}}_{=:u}, \tag{10}$$

where $x^\top := \begin{bmatrix} i^\top & v_{\mathrm{PCC},f}^\top & i_r^\top & v_{\mathrm{PCC}}^\top \end{bmatrix} \in \mathbb{R}^8$ is the state of the system. The current reference i_r and PCC voltage v_{PCC}, although considered constant, are included in the

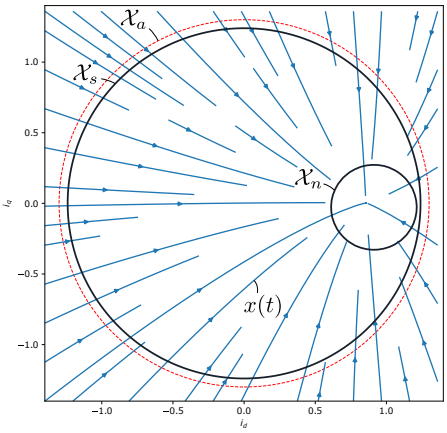

Fig. 4. The polynomial CBF and CLF, along with the corresponding safe set $\mathcal{X}_s \subsetneq \mathcal{X}_a$ and nominal region $\mathcal{X}_n$, are computed using SOS optimization. The vector field $\dot{x} = f(x) + G(x)u_{\mathrm{SOS}}(x)$, projected to (i_d, i_q) coordinates setting $(i_{r,d}, i_{r,q}) = (0, 1)$, is depicted in blue.

system dynamics to render the safety filter parametric in these variables. The set of allowed states is defined by the maximum allowed current:

$$\mathcal{X}_a = \left\{x \mid \text{subject to (9)}\right\}. \tag{11}$$

The input constraint set resulting from (1) is given as:

$$\mathcal{U} = \left\{u \mid v_{c,d}^2 + v_{c,q}^2 \leq \left(m^{\max}\right)^2\right\}, \tag{12}$$

where dc-link voltage is assumed to be $v_{dc} = 1$p.u. All parameter values can be found in Table I.

A. Control Barrier and Lyapunov-like Function

The construction of the advanced safety filter relies on the development of a CBF and CLF, which are reviewed in this subsection. We consider an abstract polynomial control system, affine in the control action $u \in \mathbb{R}^m$, and given as

$$\dot{x} = f(x) + G(x)u, \tag{13}$$

where $x \in \mathbb{R}^n$, $f(x) \in R[x]^n$ is a polynomial vector, and $G(x) \in R[x]^{n\times m}$ is a polynomial matrix. System (13) with a polynomial state feedback control policy $u_s(x) \in R[x]^m$ results in the closed-loop system

$$\dot{x} = f(x) + G(x)u_s(x). \tag{14}$$

A subset $\mathcal{X}_s \subseteq \mathbb{R}^n$ is called *forward invariant* (cf. [14, Theorem 4.4]) with respect to system (14) if for every $x(0) \in \mathcal{X}$, $x(t) \in \mathcal{X}$ for all $t \geq 0$. A system (14) is called *safe* (cf. [15]) w.r.t. an allowable set $\mathcal{X}_a \subseteq \mathbb{R}^n$ and the safe set $\mathcal{X}_s \subseteq \mathbb{R}^n$, if $\mathcal{X}_s$ is forward invariant and $\mathcal{X}_s \subsetneq \mathcal{X}_a$.

Safety of a control system (13) can be asserted with the existence of a differentiable function $B : \mathbb{R}^n \to \mathbb{R}$ such that for all states $x \in \partial\mathcal{X}_s$ there exists $u \in \mathcal{U}$:

$$\nabla B(x)^\top \left(f(x) + G(x)u\right) \leq 0. \tag{15}$$

Such a function $B(x)$ is called a Control Barrier Function (CBF), and its zero-sublevel set $\mathcal{X}_s := \{x \mid B(x) \leq 0\}$, to be contained in $\mathcal{X}_a$ (11), defines the safe set.

The advanced safety filter $u_s(x)$ ensures a finite-time convergence to the nominal region using a differentiable function $V : \mathbb{R}^n \to \mathbb{R}$ with a strictly positive dissipation rate $d(x) > 0$ such that for all $x \in \mathcal{X}_t := \{x \mid V(x) \leq x \leq B(x)\}$ there exists $u \in \mathcal{U}$ (cf. [13]):

$$\nabla V(x)^\top \left(f(x) + G(x)u\right) + d(x) \leq 0. \tag{16}$$

Such a function $V(x)$ is referred to as a Control Lyapunov-Like Function (CLF), and its zero-sublevel set $\mathcal{X}_n := \{x \mid V(x) \leq 0\} \subsetneq \mathcal{X}_s$ defines the nominal region. To ensure compatibility with the nominal controller, we furthermore require that (16) holds on the boundary of $\mathcal{X}_n$ with $u = u_n(x)$, see [13] for details. That is for all $x \in \partial X_n$:

$$\nabla V(x)^\top \left(f(x) + G(x)u_n(x)\right) + d(x) \leq 0. \tag{17}$$

With these conditions established, we can formulate the QCQP defining the advanced safety filter.

B. Quadratically Constrained Quadratic Program

When provided with a CBF $B(x)$ and a CLF $V(x)$ that satisfy conditions (15)–(17), the advanced safety filter can be implemented using the QCQP

$$\begin{aligned} u_s(x) := \quad & \min_{u\in\mathcal{U}} \quad \|u_n(x) - u\|^2 \\ & \text{s.t.} \quad C(x)u + b(x) \leq r(x), \end{aligned} \tag{18}$$

encoding the input constraint set $\mathcal{U}$ in (12) as a quadratic constraint of the QCQP. The nominal controller

$$u_n(x) = \begin{bmatrix} Z_c i_r + v_{\mathrm{PCC},f} \\ (1/\tau)(v_{\mathrm{PCC}} - v_{\mathrm{PCC},f}) \end{bmatrix} \tag{19}$$

incorporates the behavior of the simplified EDPC (6) and the nominal rate of the filtered PCC voltage (8). The state-dependent matrix $C(x) \in \mathbb{R}^{2\times 4}$ and vector $b(x) \in \mathbb{R}^2$ encode the CBF and CLF conditions (15) and (16), ensuring safety w.r.t. $\mathcal{X}_s$ and finite-time convergence to $\mathcal{X}_n$ (see [13, Lemma 1] for details):

$$C(x) := \begin{bmatrix} \nabla B(x)^\top G(x) \\ \nabla V(x)^\top G(x) \end{bmatrix} \tag{20a}$$

$$b(x) := \begin{bmatrix} \nabla B(x)^\top f(x) \\ \nabla V(x)^\top f(x) + d(x) \end{bmatrix}. \tag{20b}$$

By assuming a non-poistive values for states within $\partial\mathcal{X}_s$ and $\mathcal{X}_t$, the state-dependent slack variables $r(x) := \begin{bmatrix} r_0(x) & r_1(x) \end{bmatrix}^\top$ ensure the satisfaction of CBF and CLF conditions respectively. Furthermore, by choosing them smoothly, we can achieve a Lipschitz-continuous QCQP-based controller, see [13, Theorem 2] for details.

C. Sum-of-Squares Optimization

A polynomial CLF and CBF can be found numerically using SOS optimization. The CBF and CLF conditions (15)–(17), along with the input constraints and containment conditions $\mathcal{X}_n \subsetneq \mathcal{X}_s \subsetneq \mathcal{X}_a$, are represented as SOS constraints. This is achieved by replacing the input vector u with a polynomial controller $u_{\mathrm{SOS}}(x)$ in (15) and (16).

The SOS constraints encoding (15)–(17) are derived using Putinar's Positivstellensatz [13, Eq. (27)]:

$$\nabla B^\top (f + Gu_{\mathrm{SOS}}) + \gamma_B B + \gamma_1 f_{\mathrm{op}} \in -\Sigma[x] \quad (21a)$$

$$\nabla V^\top (f + Gu_{\mathrm{SOS}}) + d + \gamma_V V - \gamma_r B + \gamma_2 f_{\mathrm{op}} \in -\Sigma[x] \quad (21b)$$

$$\nabla V^\top (f + Gu_n) + d + \gamma_n V + \gamma_3 f_{\mathrm{op}} \in -\Sigma[x], \quad (21c)$$

for some $\gamma_B, \gamma_n \in R[x]$, and $\gamma_V, \gamma_r, \gamma_1, \gamma_2, \gamma_3 \in \Sigma[x]$, where $\Sigma[x]$ refers to the set of SOS polynomials. An operational region $\mathcal{X}_{\mathrm{op}}$, defined by the scalar function $f_{\mathrm{op}} \in R[x]$, is established to encode the considered operational ranges of the constant states i_r and v_{PCC}, where conditions (15)–(17) are expected to hold, and to ensure compactness of $\mathcal{X}_a \cap \mathcal{X}_{\mathrm{op}}$ required for Putinar's Positivstellensatz.

We propose two measures to improve control robustness with respect to time discretization effect and the use of the simplified grid and EDPC model (cf. Section II-C):

- Introduce a margin between $\mathcal{X}_a$ and $\mathcal{X}_s$.
- Adjust the nominal controller $u_n(x)$ used for the SOS constraints in (21c) to further expand the volume of the nominal region $\mathcal{X}_n$.

The resulting robust advanced safety filter maintains safety guarantees even under more complex grid models and exhibits significantly smoother behavior as it transitions into the nominal region and eventually steady-state operations.

Remark 1: The second measure mitigates instability arising from the interaction with the outer PI control loop (4) *by keeping the safety filter inactive within a larger set of states. However, utilizing an adjusted nominal controller may introduce chattering when deploying the safety filter due to violations of the compatibility condition in* (17).

IV. Numerical Results

A. Finding CBF and CLF via SOS optimization

The safe set $\mathcal{X}_s$ and nominal region $\mathcal{X}_n$, as shown in Figure 4, are computed by using polynomials $B(x)$ and $V(x)$ of degree two. Considering the linearity of the system dynamics (10) and the quadratic nature of the constraints, it is possibly expected that low-degree polynomial candidates are sufficient to find solutions to the SOS problem involving (21), though it's not perfectly obvious since (21) are still coupled quadratic equations. The CBF is selected such that $B(0) = -1$ to ensure numerical stability. The dissipation function in (16) is designed to achieve the desired convergence to the nominal region. The operational region

$$\mathcal{X}_{\mathrm{op}} = \{x \,|(i_{r,d}/i_r^{\mathrm{lim}})^2 + (i_{r,q}/i_r^{\mathrm{lim}})^2 \leq 1 \\ (v_{\mathrm{PCC},d}/0.1)^2 + (v_{\mathrm{PCC},q}/0.1)^2 \leq 1\}$$

is defined to include the operational ranges of the constant states i_r and v_{PCC}. To introduce a margin between $\mathcal{X}_a$ and $\mathcal{X}_s$ (cf. Section III-C) and to maintain compactness of the safe set w.r.t. $v_{\mathrm{PCC},f}$, we enforce the subset condition:

$$\mathcal{X}_s \subseteq \{x \,|(i_d/i^{\mathrm{lim}})^2 + (i_q/i^{\mathrm{lim}})^2 \leq 1 \\ (v_{\mathrm{PCC},f,d}/20)^2 + (v_{\mathrm{PCC},f,q}/20)^2 \leq 1\} \subsetneq \mathcal{X}_a, \quad (22)$$

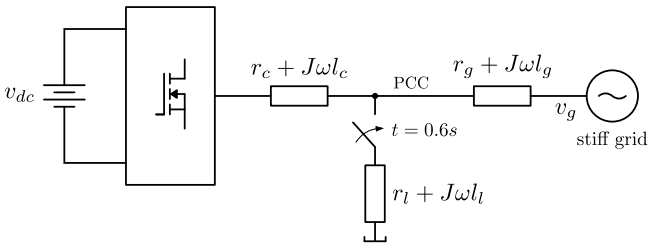

Fig. 5. Simulations are conducted by switching a load to the PCC, necessitating the limitation of the BESS's current.

TABLE I
Simulation parameters

Parameter	Symbol	Value	Unit
Transformer impedance	l_c, r_c	0.16, 0.01	p.u.
Line impedance	l_g, r_g	0.016, 0.001	p.u.
Load impedance	l_l, r_l	0.016, 0.001	p.u.
Grid voltage source	$\hat{v}_g$, f_g	1.1, 1.02	p.u.
Maximum allowed current	$i^{\max}$	1.30	p.u.
Current limits	i_r^{lim}, i^{lim}	1.18, 1.24	p.u.
Modulation limit	$m^{\max}$	1.2	p.u.
Frequency and Voltage droop	D_f, D_v	-0.02, 0.05	p.u.
Proportional gain	K_p	0.45	p.u.
Integral time constant	T_i	40	ms
Low-pass filter time constant	τ	1	ms

where $i^{\mathrm{lim}} < i^{\max}$ represents the current limit, encoding the margin. Furthermore, the nominal controller used in the SOS optimization (21) is adjusted to be more aggressive:

$$u_n(x) = \begin{bmatrix} 0.2(i_r - i) + Z_c i_r + v_{\mathrm{PCC},f} \\ 10 \cdot (1/\tau)(v_{\mathrm{PCC}} - v_{\mathrm{PCC},f}) \end{bmatrix}.$$

A more aggressive nominal controller, while potentially sacrificing condition (17), provides flexibility to increase the nominal set $\mathcal{X}_n$. The full code used for optimization and simulations is available online[1].

B. Load step simulation

In this section, we investigate the behavior of the EDPC in combination with a current limiting control – either via the vector current control or the safety filter – during a load step applied at the PCC at $t = 0.6$s, as illustrated in Figure 5. The parameter values of the electrical grid, the input constraints (1), the EDPC controller described in (3) and (4), and the current limits specified in (5), (9) and (22) are summarized in Table I. The QCQP-based controller $u_s(x)$ in (18), theoretically continuous in time, is implemented discretely with a sampling time of $T_s = 200\mu s$. The slack variables in (20) are selected as follows:

$$r_0(x) := -\gamma_B(x)B(x) \quad r_1(x) := -\gamma_V(x)V(x),$$

where γ_B and γ_V are taken from the SOS problem (21). The performance of the safety filter implementation is evaluated against the standard vector current control [4]. In this method, the vector current control is activated whenever the current amplitude $\|i\| = \sqrt{i_d^2 + i_q^2}$ exceeds the current limit

[1]https://github.com/MichaelSchneeberger/advanced-safety-filter-bess/

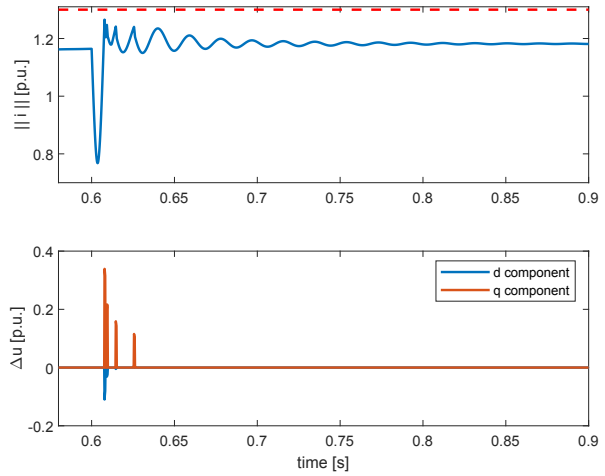

Fig. 6. The vector current control [4] is activated when the current amplitude $\|i\| \geq i^{\lim}$, with a deactivation hysteresis of 0.03 p.u. This results in abrupt interventions and a chattering behavior until the current oscillations are sufficiently reduced to remain below the current limit.

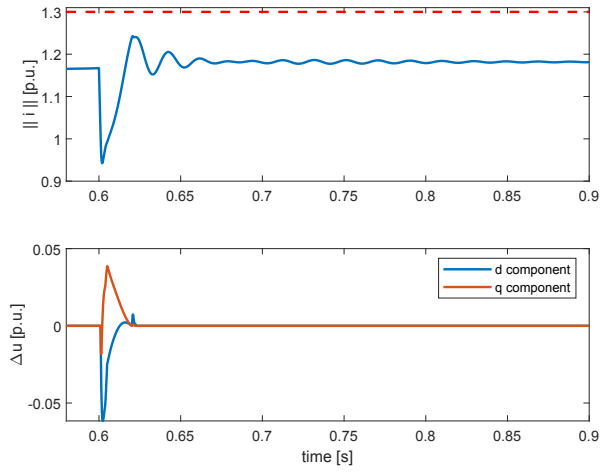

Fig. 7. The designed safety filter not only smoothly limits the current amplitude $\|i\|$ but also mitigates the current dip occurring immediately after the load step at $t = 0.6$s, facilitating a rabid return to EDPC operation.

$i^{\lim}$, with a deactivation hysteresis of 0.03 p.u. The grid's voltage amplitude and frequency is set to $\hat{v}_g = 1.1$ p.u. and $f_g = 1.02$ p.u., respectively, resulting in a maximum current reference of $\|i_r\| = i_r^{\max}$ due to the droop of the EDPC (3).

The simulations in Figures 6 and 7 show the current norm, as well as the intervention on the nominal control given by $\Delta u(x) := u_s(x) - u_n(x)$ during a load step using a vector current control and a safety filter respectively. The load step causes current oscillations that the slow EDPC cannot sufficiently mitigate, potentially leading to system shutdown due to overcurrent. To prevent this, the current limiting control – either through the vector current control or the safety filter – is activated. Unlike the vector current control, which tends to exhibit abrupt interventions and a chattering behavior even with the use of a hysteresis, the safety filter demonstrates a significantly smoother operation while keeping the current within the allowed limits. This smooth operation is achieved by means of two key conditions. Firstly, the finite-time convergence condition imposed by CLF dynamically adjusts the nominal control action to reduce the current dip immediately after the load step. Secondly, the safety condition imposed by CBF dynamically adjusts the nominal control action as the current approaches the allowed current amplitude $i^{\max}$ (9). The intervention of the safety filter, as expressed by Δu, exhibits a significant smaller magnitude and a smoother nature when compared to the vector current control.

V. Conclusions

In this paper, we demonstrated our advanced safety filter and extended the application of safety filters to a non-trivial power electronics example beyond their traditional domain in robotics. The finite-time convergence guarantee of the advanced safety filter played a key role in finding the balance between ensuring the system's safety and maintaining the behavior of the nominal controller. Specifically, we successfully implemented an advanced safety filter capable of effectively limiting the current during a load step while preserving its GFM behavior, embodied by the EDPC, during stationary grid conditions.

References

[1] Anubhav Jain, Jayachandra Naidu Sakamuri, and Nicolaos Antonio Cutululis. Grid-forming control strategies for black start by offshore wind power plants. *Wind Energy Science*, (4), 2020.

[2] Roberto Rosso, Xiongfei Wang, Marco Liserre, Xiaonan Lu, and Soenke Engelken. Grid-forming converters: Control approaches, grid-synchronization, and future trends—a review. *IEEE Open Journal of Industry Applications*, 2021.

[3] Geuss Ferdinand. Designing a controller for Walenstadt's battery energy storage system in islanded grid. Master's thesis, 2023.

[4] Mario Ndreko, Sven Rüberg, and Wilhelm Winter. Grid forming control for stable power systems with up to 100 % inverter based generation: A paradigm scenario using the IEEE 118-bus system. In *17th International Workshop on Large-Scale Integration of Wind Power into Power Systems as well as on Transmission Networks for Offshore Wind Power Plants, Sweden*, 2018.

[5] Mario Schweizer, Stefan Almér, Sami Pettersson, Arvid Merkert, Vivien Bergemann, and Lennart Harnefors. Grid-forming vector current control. *IEEE Transactions on Power Electronics*, (11), 2022.

[6] Bo Fan, Teng Liu, Fangzhou Zhao, H. Wu, and X. Wang. A review of current-limiting control of grid-forming inverters under symmetrical disturbances. *IEEE Open Journal of Power Electronics*, 2022.

[7] A.D. Ames, S. Coogan, M. Egerstedt, G. Notomista, K. Sreenath, and P. Tabuada. Control barrier functions: Theory and applications. In *2019 18th European control conference (ECC)*. IEEE, 2019.

[8] Aaron D Ames, Xiangru Xu, Jessy W Grizzle, and Paulo Tabuada. Control barrier function based quadratic programs for safety critical systems. *IEEE Transactions on Automatic Control*, (8), 2016.

[9] W. Tan and A. Packard. Searching for control Lyapunov functions using sums of squares programming. *sibi*, (1), 2004.

[10] Andrew Clark. Verification and synthesis of control barrier functions. In *2021 60th IEEE Conference on Decision and Control (CDC)*. IEEE, 2021.

[11] Han Wang, Kostas Margellos, and Antonis Papachristodoulou. Safety verification and controller synthesis for systems with input constraints. *IFAC-PapersOnLine*, (2), 2023.

[12] Hongkai Dai and Frank Permenter. Convex synthesis and verification of control-lyapunov and barrier functions with input constraints. In *2023 American Control Conference (ACC)*. IEEE, 2023.

[13] Michael Schneeberger, Silvia Mastellone, and Florian Dörfler. Advanced safety filter based on sos control barrier and lyapunov functions. *arXiv preprint arXiv:2401.06901*, 2024.

[14] H.K. Khalil. *Nonlinear Systems*. Prentice Hall, 2002.

[15] P. Wieland and F. Allgöwer. Constructive safety using control barrier functions. *IFAC Proceedings Volumes*, (12), 2007.